

Investigation into the Hydrodynamic Interaction Effects on an AUV Operating Close to a Submarine

ZQ Leong¹, KAM Saad¹, D Ranmuthugala¹, and J Duffy¹,

1. Australian Maritime College, University of Tasmania, Australia

ABSTRACT

When an Autonomous Underwater Vehicle (AUV) operates in proximity to a submarine, interaction with the flow and pressure fields of the submarine can adversely affect the motion of the AUV. This can result in mission failure, due to the AUV's inability to maintain its desired trajectory or possible collision between the two vessels.

In an aim to quantify the interaction effects and identify the regions where adverse effects of the interaction forces and moments are minimal, the Australian Maritime College (AMC) has conducted a series of Computational Fluid Dynamics (CFD) simulations and captive model experiments. The simulations were carried out on AUV and submarine models having diameter ratios between 2.237:1 and 13.425:1 at different fixed speeds and relative positions, while validation was carried out at the lower diameter ratio using the experimental results. It was found that the adverse effects of the interaction forces and moments were minimised when the AUV is around the midships of the submarine, although the actual location can change with a number of parameters such as the diameter ratio and the shape of the vehicles.

1. INTRODUCTION

In recent decades, the use of AUVs has grown significantly due to their ability to operate independent of a pilot in hazardous environments for long periods of time. This has been aided by the maturity of technologies such as power storage, navigation systems, control systems, and computational hardware which have enabled AUVs to become more cost effective and practical (Blidberg, 2001). One area that needs to be addressed is identifying the hydrodynamic interaction affecting an AUV operating in proximity to a submarine underway, as there is very little information with regard to this in the public domain, i.e. Mawby et al. (2010) and Fedor (2009).

When an AUV is operating in close proximity to a moving submarine, interaction with the submarine's wake and pressure fields can impose undesired changes to the AUV's trajectory. This can substantially hinder the approach and recovery of the AUV, and increase the risk of collision as the two vessels draw closer (Hardy and Barlow, 2008). Given that the AUV is relatively small and self-piloted by an on-board computer, the vehicle is more susceptible to the interaction effects. Therefore, it is important for AUV and submarine operators to have a good understanding of the hydrodynamic interaction between the two vessels. This will also enable designers to develop AUV controls systems to deal with the adverse interaction effects and identify operating envelopes in which an AUV can effectively manoeuvre near a moving submarine.

The authors have previously presented numerical and experimental work on the hydrodynamic interaction between an AUV and a larger diameter vehicle operating in close proximity (Mat Saad et al., 2012), with the investigation focusing on the effects of the lateral

and longitudinal distances between the two bodies at different steady state speeds. The ratio of the larger vehicle diameter to the smaller vehicle diameter, hereby referred to as the diameter ratio, was 2.237:1. The extent of the work and thus the results were limited in terms of the diameter ratio and the relative positions investigated.

This paper aims to complement the above work by considering additional lateral and longitudinal distances to determine the extent of the interaction effects and extending the investigation to a diameter ratio of 13.425:1, thus moving closer to that encountered in practice. The work is carried out through numerical modelling using Computational Fluid Dynamics (CFD) software to quantify the flow and pressure regimes in the interaction zone and to predict the behaviour of an AUV when operating within this zone. The CFD models were validated and supplemented through Experimental Fluid Dynamics (EFD) work carried out in the Towing Tank at the Australian Maritime College (AMC).

2. INVESTIGATION PROGRAMME

The interactions between the two underwater bodies were investigated through CFD and EFD work for a diameter ratio of 2.237:1 and through CFD for a diameter ratio of 13.425:1, at different longitudinal and lateral distances, and a range of speeds. The smaller AUV was represented by a 0.357:1 scaled model of the axisymmetric SUBOFF submarine hull form (Groves et al., 1989) developed by the Defence Advanced Research Projects Agency (DARPA). The CFD model of the SUBOFF included the ‘sting’ mounting arrangement in order to assist with the validation against experiment data. Due to the sting, the tail of the SUBOFF model was ‘cut off’ resulting in a length of 1.438m compared to original overall length of 1.556m. The larger body geometry, designated NP01, was a 0.587:1 scaled model of the 5m Explorer AUV designed by International Submarine Engineering (2004).

Figure 1 shows the two geometries, with the principal dimensions for the 2.237:1 diameter ratio, including the longitudinal and lateral separations. The variables investigated included the length based coefficients of the drag force, sway force, and the yaw moment acting on the SUBOFF geometry, with the latter calculated at a reference point located at 0.719m aft of the SUBOFF geometry bow tip. The lateral distance was taken as the separation gap between the two bodies while the longitudinal distance was measured from the nose tip of the larger vehicle to that of the smaller vehicle, with a ‘positive’ distance signifying that the SUBOFF is located in front of the larger vehicle. The longitudinal and lateral distances are non-dimensionalised as follows:

$$\text{Longitudinal Distance Ratio, } R_{\text{Long}} = \frac{\text{Distance SUBOFF nose tip to origin}}{L_{\text{NP01}}} \quad (1)$$

$$\text{Lateral Distance Ratio, } R_{\text{Lat}} = \frac{\text{Lateral Separation Gap}}{D_{\text{NP01}}} \quad (2)$$

In order to examine the influence of the diameter ratio on the interaction, the numerical work was carried out at two diameter ratios, i.e. 2.237:1 and 13.425:1, which was achieved by scaling up the NP01 from a diameter of 0.405m for the 2.237:1 ratio to a diameter of 2.430m for the 13.425:1 ratio, while maintaining the SUBOFF at a constant diameter of 0.181m. The length to diameter ratios of the SUBOFF and NP01 were maintained at 7.945 and 7.247, respectively.

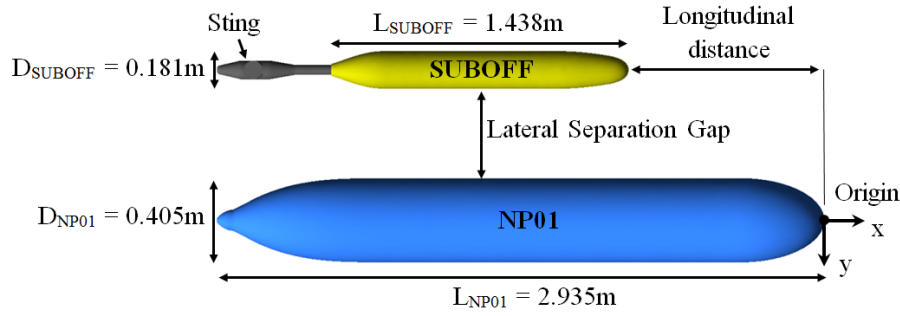


Figure 1 The 2.237:1 diameter ratio arrangement for both CFD and EFD

A summary of the test parameters, including the longitudinal and lateral separations, are given in Table 1 and in Figure 2. Since the objective of the work was to investigate the behaviour of the smaller vehicle due to the interaction, the length of the SUBOFF model (1.438m) was used as the characteristic length scale for both the Reynolds number and non-dimensionalisation of the hydrodynamic forces and moments.

Table 1 Summary of model parameters

2.237:1 Diameter Ratio (CFD and EFD)		
	Units	Descriptions
SUBOFF	m	diameter: 0.181, length: 1.438
NP01	m	diameter: 0.405, length: 2.935
Speed	m/s	0.750, 1.000, 1.500
Reynolds number _(SUBOFF Length)	- ($\times 10^6$)	1.208, 1.611, 2.416
13.425:1 Diameter Ratio (CFD)		
SUBOFF	m	diameter: 0.181, length 1.438
NP01	m	diameter: 2.430, length 17.610
Speed	m/s	1.000
Reynolds number _(SUBOFF Length)	- ($\times 10^6$)	1.611

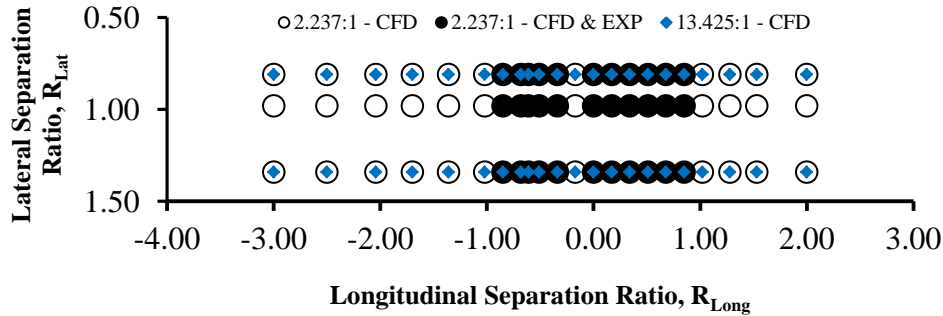


Figure 2 Configurations investigated for the diameter ratios of 2.237:1 and 13.425:1

3. NUMERICAL SIMULATION

In the 2.237:1 diameter ratio investigation, the computational fluid domain was given the same dimensions as the AMC's towing tank in order to assist with the validation of the CFD results against the experimental data. Thus the domain, shown in Figure 3, was 3.550m wide and 1.500m high, with the length kept at 40m to capture the wake field generated by the vehicles. Both vehicle models were submerged at mid-depth of the tank. The NP01 had a fixed lateral distance of 1.05m to the nearest side wall and was shifted longitudinally to achieve the desired R_{Long} . The SUBOFF was shifted laterally to achieve the desired R_{Lat} . For the 13.425:1 diameter ratio investigation, the numerical fluid domain and the NP01 were scaled up by a factor of six.

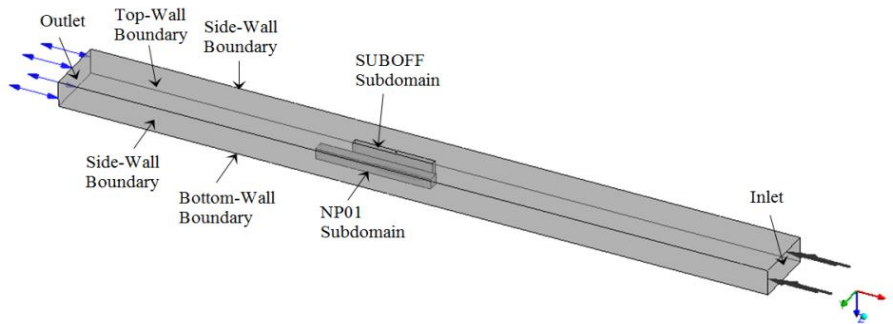


Figure 3 Computational fluid domain

The simulations were conducted on ANSYS CFX software utilising the RANS-based Baseline Reynolds Stress turbulence Model (BSLRM). Previous work on underwater vehicles (Leong, 2012) has identified through CFD and EFD work that the BSLRSM model offers more accurate predictions of forces and moments acting on similar geometries due to its ability to better model rotational flow and flow separation compared to RANS-based eddy-viscosity models. The maximum y^+ of the first mesh layer around the vehicles for the various simulation runs were maintained below two. The total thickness of the inflation layers around the SUBOFF was matched to Prandtl's theoretical estimate of turbulent boundary layer thickness over a flat plate, i.e. $0.16L_S/Re_{L_S}^{1/7}$ (White, 2011), where L_S is the surface length of the vehicle. The surface length was used instead of the overall length of the vehicle to account for the effects of surface curvature on the boundary layer thickness (Sun, 2006). The authors presented details on the grid independence and mesh refinement study in Mat Saad et al. (2012), thus only a brief discussion is provided below. An example of the refined 2.237:1 mesh is shown in Figure 4.

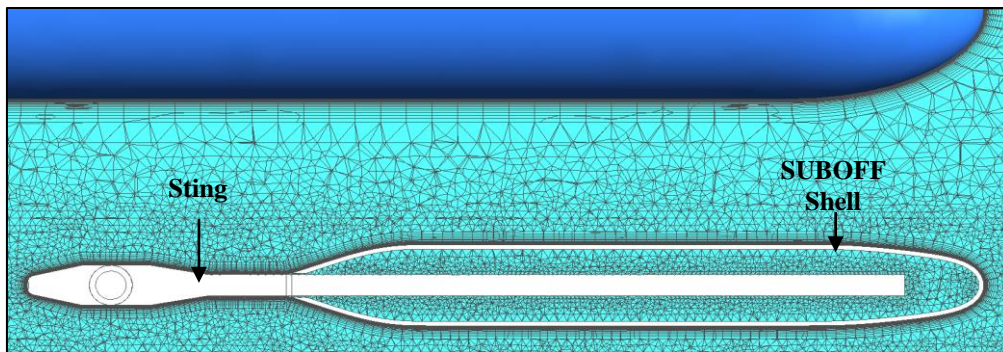


Figure 4 Mesh domain of the 2.237:1 diameter ratio model

3.1 Mesh Independence Study

The mesh independence study shown here was conducted at a speed of 1.500m/s ($Re_{SUBOFF} = 2.416E+6$), with the SUBOFF fixed at longitudinal and lateral separation ratios of -0.51 and 1.34 respectively. The mesh refinement was carried out on the surface mesh and the pressure interaction region between the vehicles. Figures 5 and 6 show the drag and sway forces, respectively, as a function of mesh size for both the 2.237:1 and 13.425:1 simulations. It is seen that above 2 million and 3 million elements for the 2.237:1 and 13.425:1 simulations respectively, the drag and side forces are relatively independent of the mesh size and were found to be within 5% of the finest mesh investigated. As a conservative measure, the 6 million elements and 8 million elements mesh models were used for the 2.237:1 and 13.425:1 diameter ratio simulations, respectively, as they were well within 1% of the force

predictions of the finest mesh investigated and provided good flow visualisation to assist with the interpretation of the results.

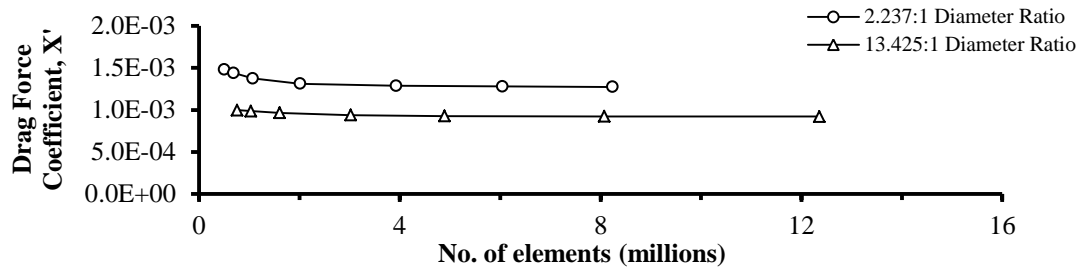


Figure 5 Grid independence study of the drag force for the diameter ratios of 2.237:1 and 13.425:1

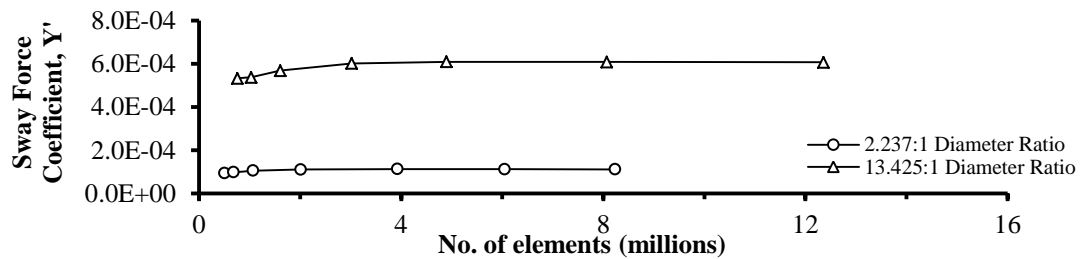


Figure 6 Grid independence study of the sway force for the diameter ratios of 2.237:1 and 13.425:1

4. EXPERIMENTAL WORK AND VALIDATION

The experiments were conducted in the Towing Tank at AMC using the 0.357:1 scaled SUBOFF model fitted with a six degrees of freedom internal load balance as shown in Figure 7(a). The experiments were only carried out for the 2.237:1 diameter ratio due to limitations on the physical sizes of the models in relation to the dimensions of the Towing Tank. The SUBOFF model had to be sufficiently large to accommodate the force balance and provide sufficient force and moment magnitudes to record meaningful data, while both captive models had to be sufficiently small to fit within the towing tank without causing excessive blockage or encroaching into the boundary layer regions of the tank. Although the 2.237:1 diameter ratio reduces the dominance of the larger vehicle on the flow and pressure regime and the resulting behaviour of the smaller SUBOFF model, it was reasoned that good agreement between experimental and CFD results at the 2.237:1 diameter ratio provides sufficient validation for the CFD model to be extended to a 13.425:1 diameter ratio.

For the validation of the CFD model, the experiments were conducted under steady-state conditions, i.e. the vehicles were moved together at constant speed, with the load balance within the SUBOFF model recording the forces and moments acting on the smaller AUV. Figure 7(b) shows the SUBOFF model located adjacent to the larger NP01. The forces on the latter were not recorded as the objective of the work was to investigate the behaviour of the smaller vehicle due to the interaction. The estimated uncertainty for the measured force coefficient was 1.191E-04 for a single run, based on the recommended analysis procedure outlined in ITTC (2002).

Examples of the validation process are shown in Figures 8 and 9, where a comparison between the CFD and EFD results are provided for the drag and side force coefficients of the

SUBOFF respectively, as the longitudinal separation is varied at two different lateral separations. The figures show good agreement between the results, with the difference being less than the experimental uncertainty, and both results displaying similar trends. Similar comparisons were made for different configurations and speeds, enabling the CFD model to be validated and used as an investigation tool.

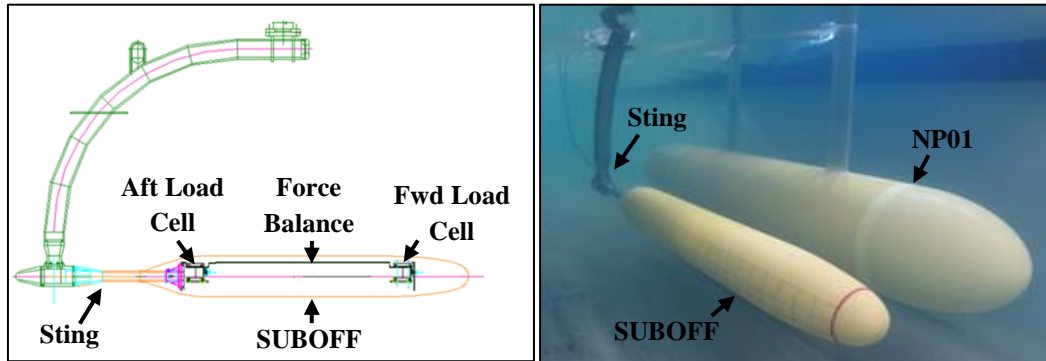


Figure 7 (a) SUBOFF testing rig (b) SUBOFF located adjacent to NP01

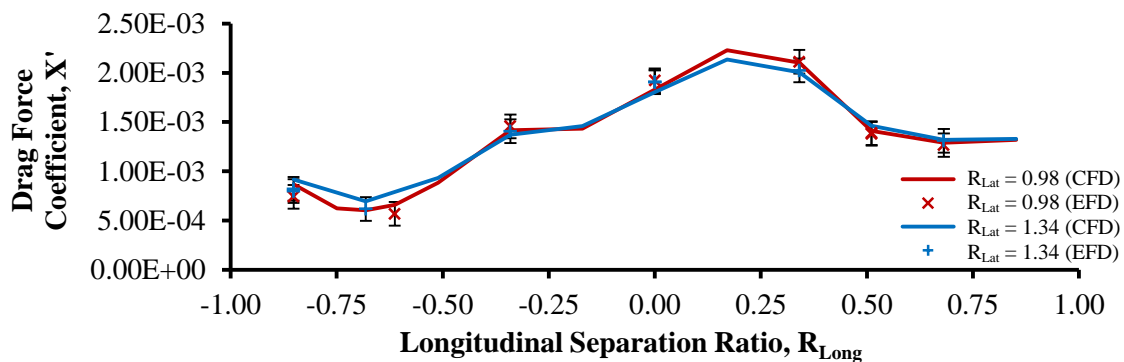


Figure 8 Drag force coefficient vs R_{Long} at $Re_{SUBOFF} = 1.611 \times 10^6$ (2.237:1 diameter ratio), error bars of the experimental results are at a value of $1.191E-04$

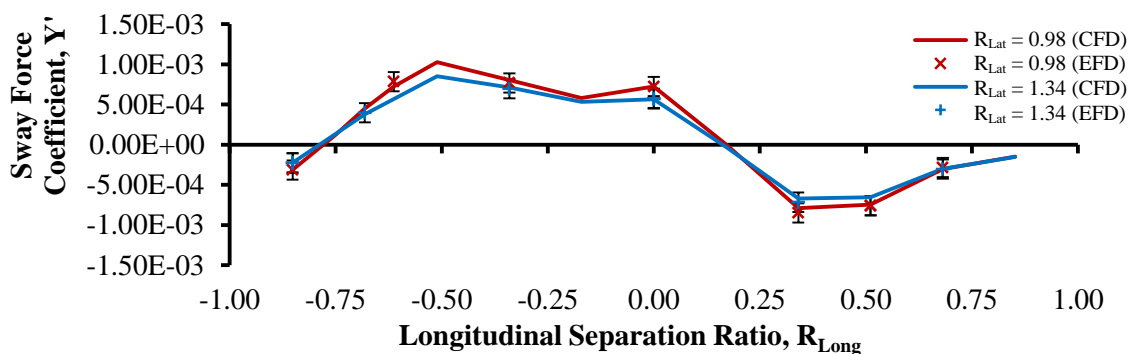


Figure 9 Sway force coefficient vs R_{Long} at $Re_{SUBOFF} = 1.611 \times 10^6$ (2.237:1 diameter ratio), error bars of the experimental results are at a value of $1.191E-04$

5. RESULTS AND DISCUSSION

Given that the study investigated the hydrodynamic coefficients of an AUV in close proximity to a moving larger body, as the longitudinal and lateral separations between them and the forward speed were varied, it resulted in a significant quantity of data representing the combination of numerical and experimental runs. Thus the following discussion will focus on selected combinations as examples of the results analysed.

Figure 10 gives the yaw moment coefficient acting on the SUBOFF for various longitudinal separation ratios for the 2.237:1 diameter ratio. It was observed that at a R_{Long} of -1.00, the SUBOFF starts to experience a moment that tends to yaw its bow towards the NP01. The moment is due to the SUBOFF bow interacting with the low pressure around the NP01 stern as shown in Figure 12. The moment peaks is at a R_{Long} of -0.70, which decreases thereafter due to the negative pressure region around the NP01 midsection affecting the whole length of the SUBOFF (see Figure 12), which also acts to attract the two bodies together (see Figure 11). A small region where the yaw moment is small presents itself around R_{Long} of -0.34. However, the SUBOFF needs to travel only a small distance adjacent to this region for the direction of moment to change. This may lead to problems for a control system that is too sensitive, resulting in undesired oscillations if the system tries to overcompensate for the change.

When the SUBOFF is in the bow region of the larger body ($R_{Long} > -0.34$), the interaction moment starts to yaw the SUBOFF away from the NP01. It is also observed that around R_{Long} of 0.00 the sway attraction force declines rapidly and acts to strongly repel the two bodies apart (see Figure 13). Both the yaw moment and repelling (sway) force peak at around a R_{Long} of 0.17 and then gradually decreases to a negligible magnitude as the SUBOFF moves forward at around a R_{Long} of 2.00.

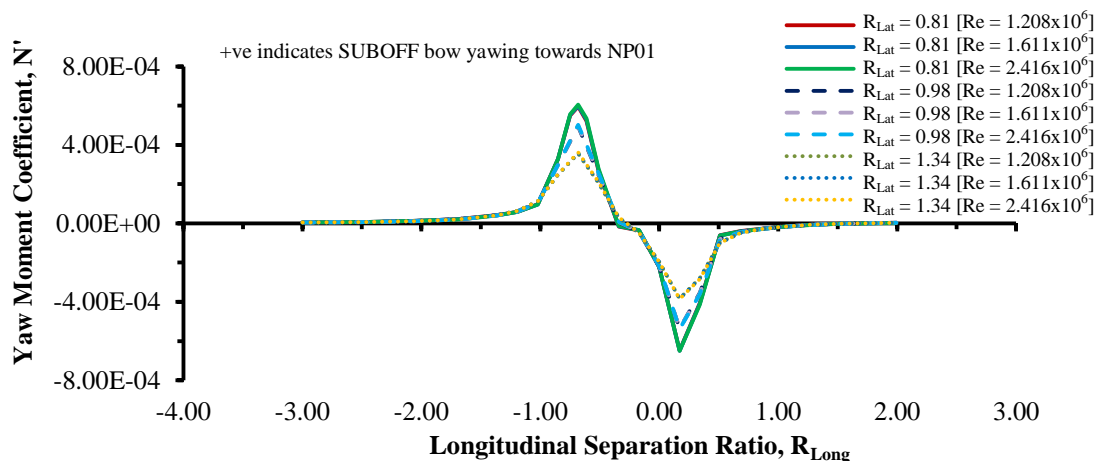


Figure 10 Yaw moment coefficient vs R_{Long} for diameter ratio of 2:237:1

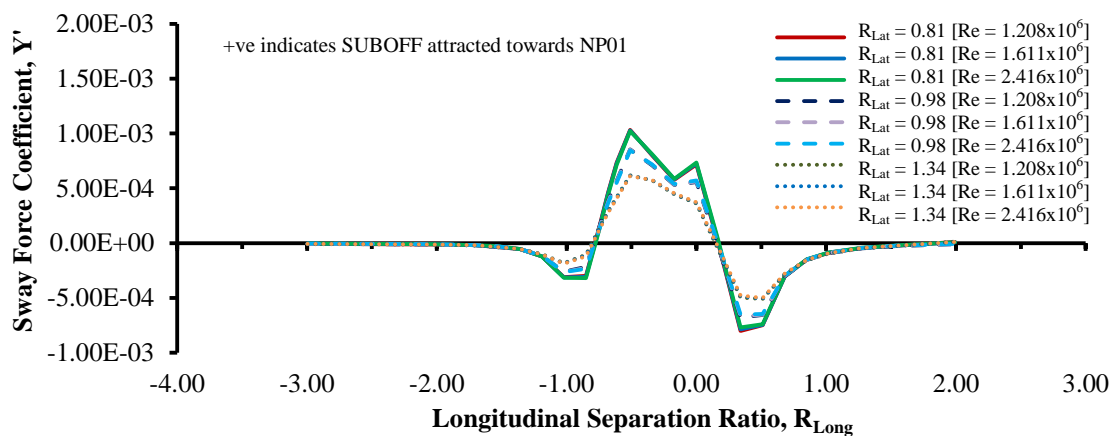


Figure 11 Sway force coefficient vs R_{Long} for diameter ratio of 2:237:1

The behaviour of the yaw moment and sway force coefficients with respect to R_{Long} as discussed above were found to be similar for the different lateral separations investigated.

The only exceptions were a decrease in the interaction magnitude as R_{Lat} increased and a ‘dip’ in the sway force at a R_{Long} of 0.17 for R_{Lat} of 0.81 and 0.98. Both the yaw moment and sway force coefficients with respect to R_{Long} were found to be relatively independent of Re , as shown in Figures 10 and 11. This suggests that test cases at one Re would be sufficient to represent the interaction behaviour of the sway force and yaw moment coefficients with respect to different longitudinal separations.

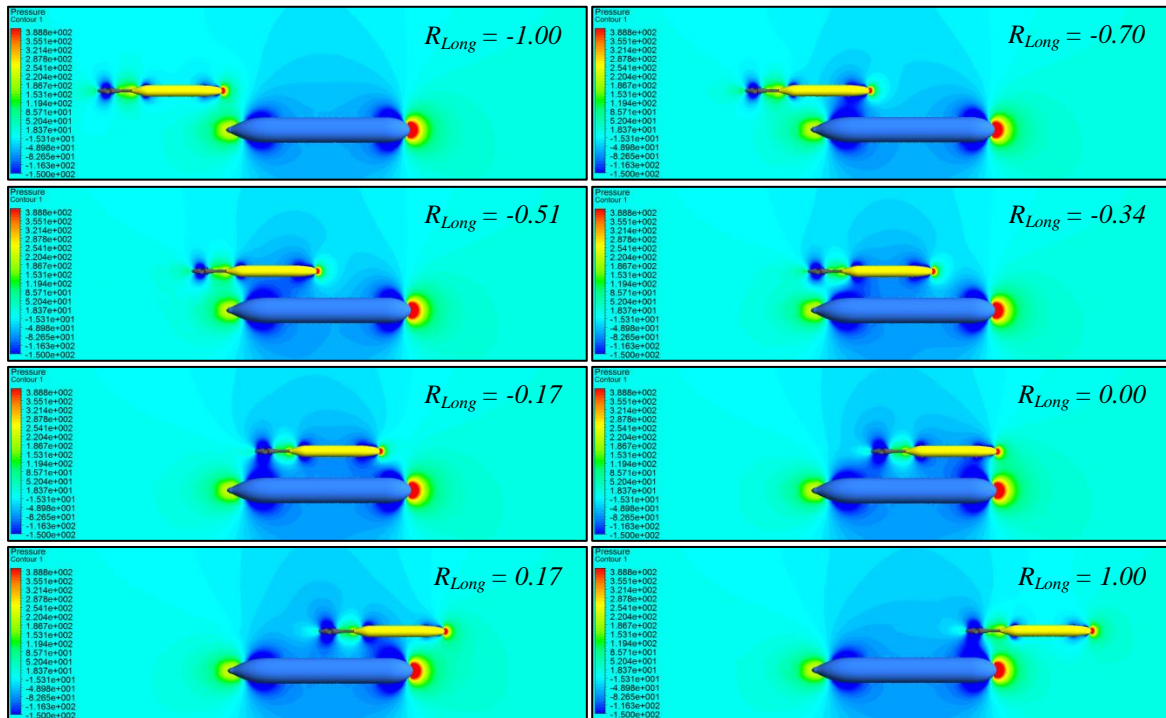


Figure 12 Pressure visualisation vs R_{Long} at $Re_{SUBOFF} = 2.416 \times 10^6$ and $R_{Lat} = 0.81$ for diameter ratio of 2:237:1

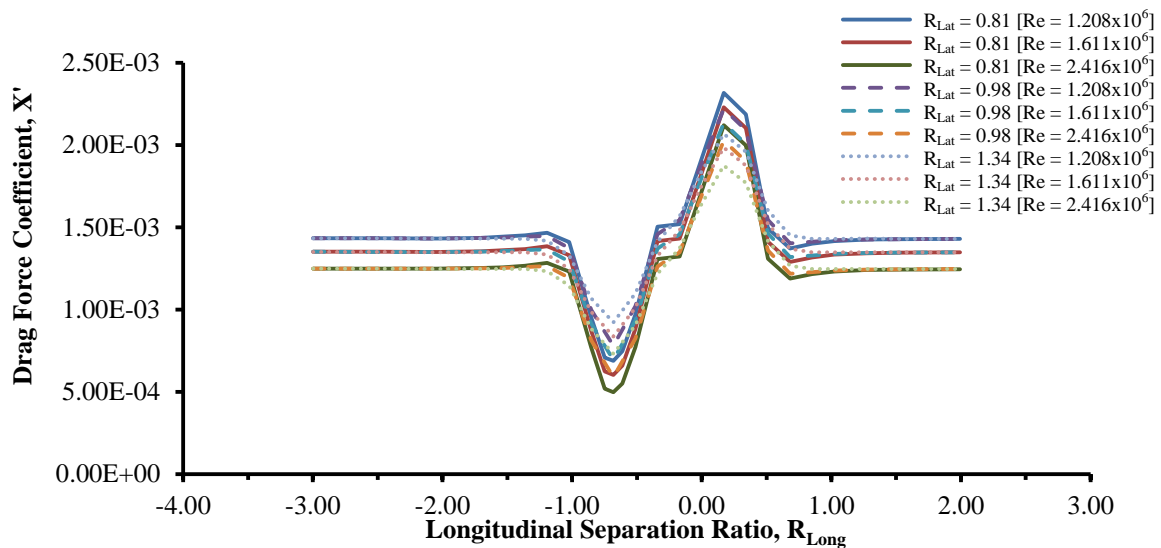


Figure 13 Drag force coefficient vs R_{Long} for diameter ratio of 2:237:1

Figure 13 gives the drag force coefficient on the SUBOFF with respect to R_{Long} , which shows that the drag force decreases when the SUBOFF is in the stern region of NP01. The drag then starts increasing beyond a R_{Long} of about -0.75, peaking at around 0.17, which then declines and recovers to the base value at around R_{Long} of 2.00. These changes are due to the pressure

variations between the vehicles whereby the SUBOFF will experience a lower drag transitioning from a higher pressure region to a lower region along the length of the NP01, and a higher drag when transitioning from a lower pressure region to a higher region along the length of the NP01. It was found that Re affects the magnitude of the interaction influence on the drag coefficient. However, the general location of its peaks and troughs with respect to R_{Long} remains reasonably constant.

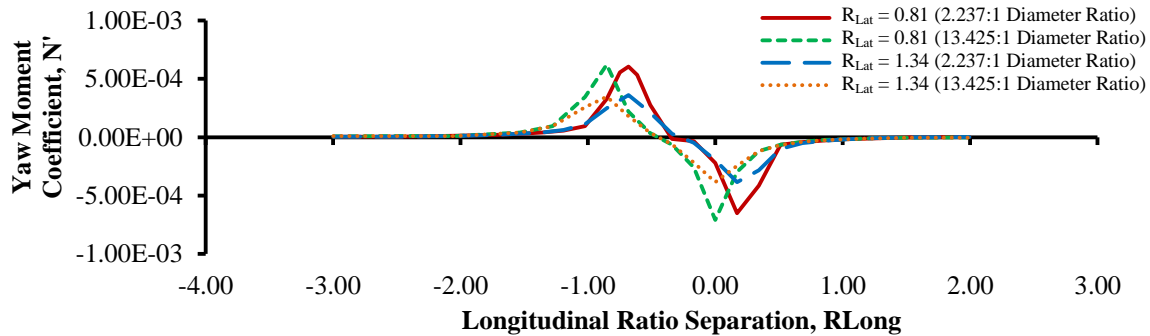


Figure 14 Yaw moment coefficient vs R_{Long} at a flow speed of $Re_{SUBOFF} = 2.416 \times 10^6$ for diameter ratios of 2:237:1 and 13.425:1

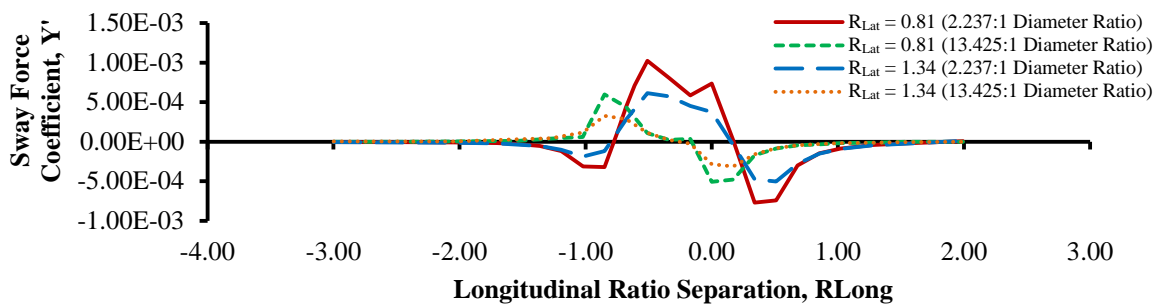


Figure 15 Sway force coefficient vs R_{Long} at a flow speed of $Re_{SUBOFF} = 2.416 \times 10^6$ for diameter ratios of 2:237:1 and 13.425:1

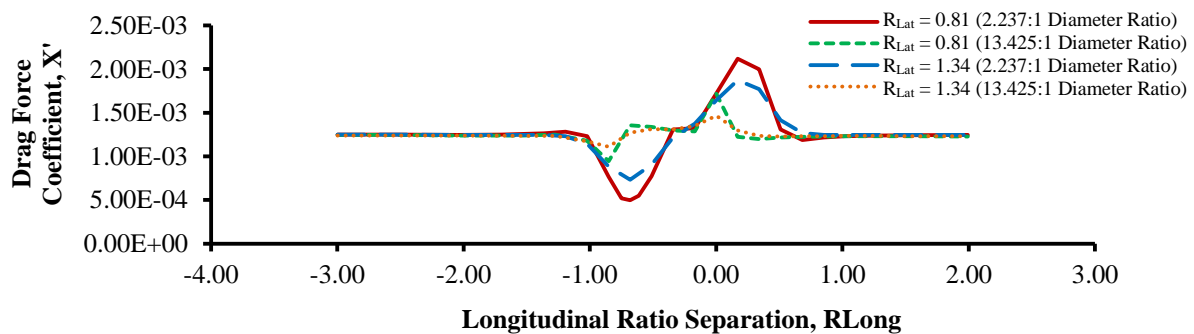


Figure 16 Drag force coefficient vs R_{Long} at a flow speed of $Re_{SUBOFF} = 2.416 \times 10^6$ and at $R_{Lat} = 1.34$ for diameter ratios of 2:237:1 and 13.425:1

Figures 14, 15, and 16 give the yaw moment, sway force and drag force coefficients respectively, for the SUBOFF with varying R_{Long} for both the 2.237:1 and 13.425:1 diameter ratio simulations at the lowest and highest R_{Lat} investigated, i.e. 0.81 and 1.34. With the 13.425:1 ratio, the observed interaction influence on the peaks and troughs of the drag force, sway force, and yaw moment were shifted further aft compared to the 2.237:1 diameter ratio. However, while the range of the interaction influence for the 13.425:1 diameter ratio was greater than that for the 2.237:1 diameter ratio, the magnitude of interaction influence on the drag force and sway force were much lower for the 13:425:1 diameter ratio. The interaction

influence on the yaw moment for the 13.425:1 diameter ratio was also found to be fairly similar in magnitude compared to the 2.237:1 diameter ratio. These observations are counterintuitive as it was expected that the 13.425:1 diameter ratio would have a higher interaction effect on the forces and moments experienced by the smaller body in proximity. This suggests that the trends at different diameter ratios should be investigated to ascertain the characteristic of the shift and magnitude of the interaction effects, to enable designers and operators to adapt based on the diameter ratio encountered. This investigation is currently being carried out.

Based on the observed trends in the results presented above, it is undesirable for an AUV to approach a larger moving body from either the bow or the stern of the latter due to the large fluctuations in the hydrodynamic interaction (especially the sway force and yaw moment) as the AUV moves along the length of the larger body. These fluctuations were however noticeably less when the AUV was around the midsection of the larger body, i.e. close to a R_{Long} of 0.5. The interaction effects were also found to be inversely proportionate to R_{Lat} . This suggests that a possible path for the AUV to approach (see Figure 17) or depart the larger body would be from the side around the midship of the latter in order to minimise the adverse effects of the interaction.

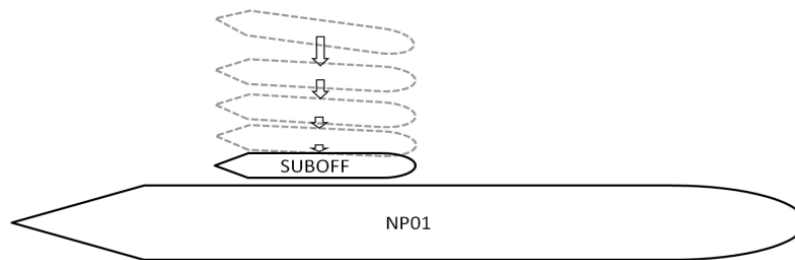


Figure 17 Relative path for the AUV to approach the larger body with minimum hydrodynamic interaction. Forward speeds of the two bodies are matching

6. CONCLUSION

This paper investigates the interaction forces and moments on an AUV when operating in close proximity to a moving submarine in order to identify regions of minimum interaction. The investigation utilised CFD and EFD techniques to obtain the forces and moments acting on the AUV due to its interaction with the flow field of the larger vehicle. The EFD results from captive model tests were used to validate a 2.237:1 diameter ratio CFD model at a number of longitudinal and lateral separations and speeds, with the CFD model modified to investigate a 13.425:1 diameter ratio configuration.

The results showed that the AUV approaching the larger body from the bow or stern poses a high risk of collision and a challenge to the control systems due to the high variation in the interaction forces between the two bodies. The results suggest a safer path would be for the AUV to approach or depart the larger vehicle from the side around the midship of the latter.

The interaction influence on the sway force and yaw moment was found to be independent of Re . Therefore, it is possible to carry out future investigations at one operational Re to represent the interaction behaviour with respect to different relative longitudinal and lateral positions. Further investigations are being undertaken to extend the current assessment of the interaction at different diameter ratios and at relative speeds between the vehicles.

7. NOTATION

D	Diameter of vehicle
L	Overall length of vehicle
L_S	Surface length of vehicle
U	Longitudinal velocity
R_{Lat}	Lateral separation ratio
R_{Long}	Longitudinal separation ratio
Re	Reynolds number
ρ	Water density
X	Drag force
X'	Non-dimensional drag force coefficient, defined as $\frac{2X}{\rho L^2 U^2}$
Y	Sway force
Y'	Non-dimensional sway force coefficient, defined as $\frac{2Y}{\rho L^2 U^2}$
N	Yaw Moment
N'	Non-dimensional yaw moment coefficient, defined as $\frac{2N}{\rho L^3 U^2}$

8. REFERENCES

1. Blidberg, D.R., (2001), "The Development of Autonomous Underwater Vehicles (AUV); A Brief Summary", Proceeding of the IEEE International Conference on Robotics and Automation, Seoul, Korea, May 2001.
2. Hardy, T., (2008), "Unmanned Underwater Vehicle (UUV) deployment and retrieval considerations for submarines", Proceedings of the 11th International Naval Engineering Conference, Hamburg, Germany.
3. Fedor, R. (2009), "Simulation of a Launch and Recovery of an UUV to a Submarine", KTH Royal Institute of Technology, Sweden.
4. Groves, N.C., Huang, T.T., and Chang, M.S., (1989), "Geometric Characteristics of DARPA SUBOFF Models (DTRC Model Nos 5470 and 5471)", David Taylor Research Centre, Bethesda, Maryland, USA.
5. International Submarine Engineering, (2004), "Explorer Autonomous Underwater Vehicle". Retrieved 02/12/2012, from www.ise.bc.ca/explorer.html.
6. ITTC, (2002), "Recommended Procedures and Guidelines: Testing and Extrapolation Methods: Resistance- Uncertainty Analysis, Example for Resistance Test", 23rd ITTC 2002, Venice, Italy.
7. Mawby, A., Wilson, P., Bole, M., Fiddes, S.P., and Duncan, J. (2010), "Manoeuvring Simulation of Multiple Underwater Vehicles in Close Proximity", United Kingdom.
8. Leong, Z.Q., and Ranmuthugala, D., (2012), "Evaluation of The Turbulence Models (BSLRSM, SST, $k-\omega$) Forces and Moments Predictions for Translation and Rotational Motion of The DAPRA SUBOFF", Australian Maritime College, Tasmania, Australia.
9. Sun, J.L., (2006), "Three-Dimensional Thick Boundary Layer Calculation of a Submarine and a Research for Two-Dimensional Free Surface Wave", Huazhong University of Science and Technology, Huazhong, China.
10. White, F.W., (2011), "Fluid Mechanics", 7th ed., McGraw-Hill, New York.